Journal of Materials Chemistry C

Accepted Manuscript

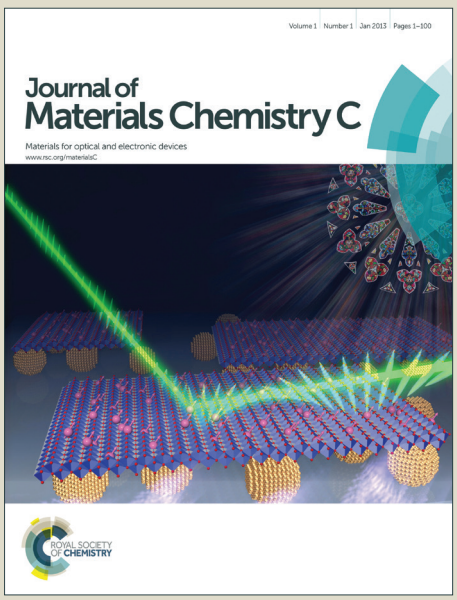

ROYAL SOCIETY OF CHEMISTRY

www.rsc.org/materialsC

Journal Name

RSCPublishing

ARTICLE

A Resonance Energy Transfer Approach for the Selective Detection of Aromatic Amino Acids

Cite this: DOI: 10.1039/x0xx00000x

Chanchal Hazra, Tuhin Samanta and Venkataramanan Mahalingam*

Received 00th January 2012,
Accepted 00th January 2012

DOI: 10.1039/x0xx00000x

www.rsc.org/

In this article, we report for the first time the use of Ln^{3+}-doped nanocrystals to detect aromatic amino acids (AAs) up to nanomolar concentration. Detection of AAs is important as the increased levels of AAs in the gastric juice samples were detected in the early phase of gastric carcinogenesis. In this work, we have shown that highly efficient energy transfer between Ce^{3+} and Tb^{3+} ions in Ce^{3+}/Tb^{3+}-doped $CaMoO_4$ nanocrystals is selectively altered with the addition of AAs thus providing a simple resonanoce energy transfer (RET) approach to detect AAs in the nanomolar (nM) range. This is achieved as the absorption spectrum of AAs overlaps with the emission spectrum of the Ce^{3+}/Tb^{3+}-doped $CaMoO_4$ nanocrystals thus reducing the energy transfer efficiency between Ce^{3+} and Tb^{3+} ions. This selective energy transfer process led to the quenching of the Tb^{3+} emission from the nanocrystals. The high selectivity was veryfied by the addition of essential or non-essential amino acids, some metal ions and molecules which are generally expected to coexist with AAs in our body. Moreover, the selective quenching of the Tb^{3+} ions emission is reversible with the addition of ninhydrin with recovery of almost 90% of the initial luminescence intensity. This process has been repeated for more than five cycles with only a slight decrease in the sensing ability. The study was also extended to the 2D surface where the nanocrystals are strongly attached to a positively charged surface which upon dipping in AAs solution lead to the quenching of Tb^{3+} ions luminescence and the same recovered after dipping in ninhydrin solution.

1 Introduction

Aromatic amino acids (AAs) i.e. tryptophan, tyrosine and phenylalanine) are of interest due to their contribution to secondary protein structure through noncovalent binding interactions.[1-5] AAs are important essential amino acids for animals to make hormones and melanine skin.[6-12] Upon UV excitation, proteins and peptides with AAs residues are intrinsically fluorescent and these residues have distinct absorption and emission wavelengths. The fluorescence spectrum of a protein containing AAs, resembles that of tryptophan due to its high molar absorptivity (5,050 $M^{-1}cm^{-1}$). Early-stage gastric cancer is mostly asymptomatic and can easily be missed by conventional gastroscopy.[13-15] To the best of our knowledge, there are no biomarkers for the early detection of gastric cancer whereas increased levels of AAs in the gastric juice samples were detected in the early phase of gastric carcinogenesis.[16-18] Therefore, determination of AAs has drawn much attention in the field of biological and clinical application.[19-21]

Quantitative determination of samples containing amino acids is possible with analytical methods like atomic absorption spectrometry (AAS), inductively coupled plasma-mass spectrometry (ICPMS), liquid chromatography/ mass spectrometry (UPLC-MS), etc.[22] Although these methods are quite sensitive they are quite expensive and time consuming. Alternatively, chemosensor based on organic molecules or metal complexes have been developed for selective detection of amino acids.[23] Although they are quite sensitive, the organic molecules are not very robust to be used in device fabrication. They also photobleach under light and this degrades their efficiency. Recently, nanoparticles have been reported as a platform to detect amino acids.[24] For example, surface plasmon frequency of metal nanoparticles (Au and Ag) have been tuned by the selective attachment of amino acids.[25] In another study, Brett and co-workers have used screen-printed electrodes for the determination of amino acids, focussing particularly on tryptophan, following different surface modifications by carbon nanotubes (CNT), carbon black (CB) and copper nanoparticles.[26] Surface modified colloidal CdS nanoparticles are found to be selective towards detection of cysteine in the

presence of other amino acids in the micromolar concentration range.[27] Mirkin and co-workers developed DNA-gold nanoparticle based colorimetric competition assay for the detection of cysteine with detection limit 100 nM.[28] In another study the visual detection of D-amino acids is achieved through the anti-aggregation of 4-mercaptobenzoic acid modified gold nanoparticles (AuNPs) in the presence of D-amino acid oxidase. The limit of detection in this method is found to be 75 nM for D-alanine.[29] Li et al. have shown CdSe quantum dot for the detection of methionine. A linear increase in the fluorescence intensity of CdSe is noted upon methionine addition in the concentration range 10^{-7} to 10^{-4} (M). The detection limit is close to 4.5 μM. In the same study for phenylalanine the detection limit was found to be 3.2 μM.[30] Although nanoparticles of gold, CdS and CdSe are quite robust, they show broad absorption thus affecting the sensitivity of the detection. Moreover, they possess size dependent optical properties thus demanding the use of monodispersed nanoparticles. Alternatively, Ln^{3+}-doped nanoparticles possess sharp luminescence signals which are less affected by the ligand environment.[31-33] In addition, they possess longer luminescence lifetime which can be used as an additional tool for the detection. Recently, there is a surge in the interest towards these nanoparticles due to their use in sensing and bioimaging applications.[34,35] To the best of our knowledge, there is only one report on the use of Ln^{3+} emission for the selective detection of amino acid. In this work quantitative detection of cysteine/homocystein is achieved using Ln-doped nanoparticles which show emission via upconversion.[36] The reported detection limit for cysteine is close to 28.5μM. Thus it is challenging to develop highly luminescent Ln-doped materials which can detect aromatic amino acids in the nM concentration range.

In this article, we have shown that the strong green emission from Tb^{3+} ions via energy transfer from Ce^{3+} ions is selectively quenched in the presence of AAs. This is achieved as the absorption of the AAs overlaps with the emission band of Ce^{3+} ions. The quenching is found to be very selective as hardly any effect of other analytes was observed. Moreover, the quenching of the Tb^{3+} emission is reversible by the addition of ninhydrin. The quenching and recovery cycles can be performed for multiple times without much reduction in the emission efficiency.

2 Experimental sections:

2.1 Materials: Tb_2O_3, $Ce(NO_3)_3.6H_2O$ (from Sigma-Aldrich), ammonium heptamolybdate tetra hydrate [$(NH_4)_6Mo_7O_{24}.4H_2O$], $CaCl_2$ (from Merck), deionizer water, 1 (M) HNO_3 (Merck, 70% pure), sodium dodecyl sulphate (SDS) from Merck were used for the synthesis. Glucose, sucrose, citric acid (from Sigma-Aldrich), KCl, $Cu(NO_3)_2.3H_2O$ (from Merck), $Zn(acac)_2.2H_2O$, $Fe(NO_3)_3.9H_2O$ (from Sigma) and tryptophan, tyrosine, phenylalanine, histidine, arginine, leucine, isoleucine, lysine, methionine, proline, glycine, alanine, cysteine, serine, ninhydrin (from SRL) were used for sensing measurements.

2.2 Synthesis:

Water dispersible Ce^{3+}/Tb^{3+}-doped $CaMoO_4$ nanocrystals were synthesized using microwave procedure. Briefly, the stoichiometric amounts of Tb_2O_3 was converted into their corresponding nitrates by dissolving in 1 M HNO_3 whereas $CaCl_2$, $(NH_4)_6Mo_7O_{24}.4H_2O$ and SDS were used as received. In a typical procedure, a $(NH_4)_6Mo_7O_{24}.4H_2O/H_2O$ stock solution was prepared by dissolving 1 mmol $(NH_4)_6Mo_7O_{24}.4H_2O$ in 25 ml H_2O at room temperature. A mixture of $CaCl_2$ (0.96 mmol, 106.58 mg), Tb $(NO_3)_3$ (0.01 mmol, 4.36 mg), $Ce(NO_3)_3$ (0.03 mmol, 13.03 mg) SDS (1 mmol, 288.38 mg) were added to 15 ml H_2O under vigorous stirring at 60° C temperature, forming a transparent solution. A 2 ml of $(NH_4)_6Mo_7O_{24}.4H_2O/H_2O$ stock solution was slowly added into the mixture and stirring was continued for another 10 min. Subsequently the transparent solution was transferred to a 10 ml vial used for microwave synthesis using Anton Parr Monowave 300 microwave reactor. The vial was tightly sealed with Teflon cap and then microwave heated at 90° C for 10 minutes. Finally, the light yellow coloured precipitate was collected by centrifugation and washed thrice with ethanol, followed by deionized water to remove any unreacted reactants.

2.3 Characterization:

The X-ray diffraction (XRD) patterns were collected using the Rigaku (Japan); SmartLab) model; diffractometer attached with D/tex ultra detector and Cu K_α source operating at 35 mA and 70 kV. Scan range was set from 10-70° 2θ with a step size of 0.02° and a count time of 2 s. The samples were well powdered and spread evenly on a quartz slide. The transmission electron microscopy (TEM) images were taken on a JEOL (Japan); JEM 2100 F model; UHR-FEG-TEM using a 200 kV electron source. Samples were prepared by placing a drop of aqueous dispersion of the nanocrystals on a carbon coated copper grid and the grid was dried under air. Room temperature optical absorption spectra of all the samples were recorded on a Hitachi (Japan); (U4100) model; spectrophotometer. The samples were taken in a 3 ml quartz cuvette (path length, 1 cm). The photoluminescence (PL) spectra were measured on a Horiba Jobin Yvon Fluorolog CP machine (USA); iHR 320 model; spectrometer equipped with 450 W Xe lamp. The excitation and emission light were dispersed using Czerny-Turner monochromator with an optical resolution of 1 nm. The emitted photons were detected using a Hamamatsu R928 detector. The output signal was recorded using a computer. The PL lifetime measurements were performed with the Horiba Jobin Yvon Fluorolog CP machine (USA); iHR 320 model; equipped with a pulsed Xe source operating at 25 W.

3 Results and Discussion:

Water dispersible Ce^{3+}/Tb^{3+}-doped $CaMoO_4$ nanocrystals were synthesized using a procedure recently developed by our

group.[37] The high dispersibility of the nanocrystals is achieved through a bilayer coating of sodium dodecyl sulphate (SDS) over the surface of the nanocrystals. The average size of the nanocrystals is ~ 100 nm and they are spherical in shape as evident from TEM image shown in Fig. 1A. The formation of tetragonal phase $CaMoO_4$ is confirmed by the XRD pattern shown in Fig. 1B along with the peaks indexed to the corresponding *hkl* planes. All diffraction peaks are matched with the standard pattern of tetragonal $CaMoO_4$ crystals.

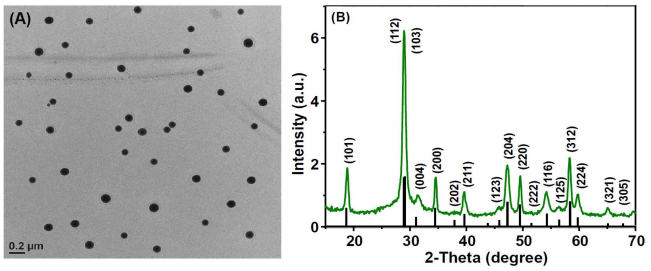

Fig.1 (A) TEM image and (B) XRD pattern of Ce^{3+}/Tb^{3+}-doped $CaMoO_4$ nanocrystals. The vertical lines in (B) is the standard XRD pattern of $CaMoO_4$ nanocrystals (ICSD PDF Card No.: 01-085-1267).

The PL and excitation spectra of 0.1 wt% Ce^{3+}/Tb^{3+}-doped $CaMoO_4$ nanocrystals are shown in Fig. 2. The excitation spectrum obtained by monitoring Tb^{3+} emission at 542 nm shows an intense broad band around 280 nm which corresponds to the transition from ground state ($^2F_{5/2}$) to the excited *4f5d* state of Ce^{3+} ions. Upon Ce^{3+} (280 nm) excitation, Ce^{3+}/Tb^{3+}-doped $CaMoO_4$ nanocrystals show strong emission at 540 nm along with weak emissions near 488, 585 and 620 nm which are assigned to $^5D_4 \rightarrow {}^7F_5$, $^5D_4 \rightarrow {}^7F_6$, $^5D_4 \rightarrow {}^7F_4$ and $^5D_4 \rightarrow {}^7F_3$ transitions, respectively. This clearly suggests an energy transfer from Ce^{3+} to Tb^{3+} ions in Ce^{3+}/Tb^{3+}-doped $CaMoO_4$ nanocrystals.[38] The luminescence lifetime of the $^5D_4$ state of Tb^{3+} ion in Ce^{3+}/Tb^{3+}doped $CaMoO_4$ nanocrystals is about 1.97 ms as calculated from the decay analysis (shown in Fig. S4). The intense luminescence signal and longer lifetime of Tb^{3+} ions in Ce^{3+}/Tb^{3+}-doped $CaMoO_4$ nanocrystals are further supported by the quantum efficiency of the nanocrystals. The calculated quantum yield is about 27% which is measured using quinine sulphate as the reference standard. The details of the measurement and calculations are given in Fig. S1.

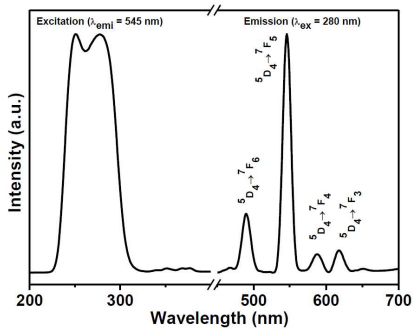

Fig.2 Photoluminescence (PL) and excitation spectra of 0.1wt% Ce^{3+}/Tb^{3+}-doped $CaMoO_4$ nanocrystals.

To investigate the sensing ability, the Ce^{3+}/Tb^{3+}-doped $CaMoO_4$ nanocrystals were exposed to the 5 X 10^{-8} (M) aqueous solution of AAs. The emission spectra shown in Fig. 3 clearly indicate that upon addition of AAs solution, the intensity of the Tb^{3+} emission decreases dramatically. To verify that the observed quenching of the Tb^{3+} emission upon addition of AAs is quite selective, we added both essential and non-essential amino acids like, histidine, leucine, isoleucine, lysine, methionine and glycine, alanine, cysteine, proline, serine and arginine with 5 X 10^{-8} (M) concentration to the nanocrystal dispersion. There is hardly any change in the intensity of the

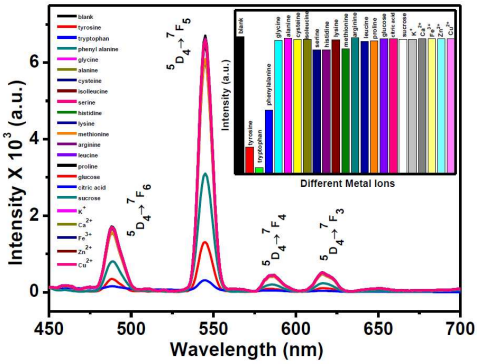

Fig. 3. PL spectra of Ce^{3+}/Tb^{3+}-doped $CaMoO_4$ nanocrystals after mixing with different analytes including AAs. Inset represents the change in the emission intensity of Tb^{3+} ions in a bar diagram.

Tb^{3+} emission is noticed. Similarly, we added other ions and molecules (having same 5 X 10^{-8} (M) concentration) such as glucose, citric acid, K^+, Fe^{3+}, Cu^{2+} which are generally expected to coexist with AAs in the body. Again, there was no change observed in the luminescence intensity of the Tb^{3+} ions. The above results are shown as bar diagram in the inset of Fig. 3.

To examine the effect of interference by other ions and molecules on the quenching of emission intensity of Tb^{3+} ions by tryptophan, a control experiment was performed where an equimolar mixture of tryptophan along with other analytes (except tyrosine and phenylalanine) were added to the aqueous dispersion of Ce^{3+}/Tb^{3+}-doped $CaMoO_4$ nanocrystals. The results indicate that quenching of the PL emission intensity by tryptophan is not affected in the presence of interfering ions and molecules (shown in Fig. 4). The results of interference study for other two AAs (tyrosine & phenylalanine) are shown in Fig. S2.

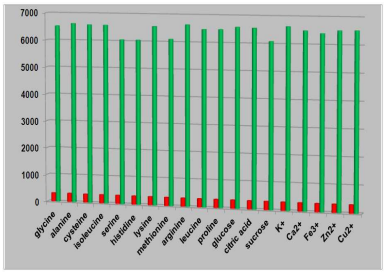

Fig. 4. Interference study of Ce^{3+}/Tb^{3+}-doped $CaMoO_4$ nanocrystals dispersion containing both tryptophan and other analytes (except tyrosine and phenylalanine).

We believe the reason for the decrease in the intensity of the Tb^{3+} emission is due to efficient energy transfer occurring between Ce^{3+} ions and AAs. This is reasonable to assume as the absorption spectra of AAs overlaps with the PL spectrum of the Ce^{3+}-doped $CaMoO_4$ nanocrystals (shown in Fig. 5). Although the overlap region is small, the absorption coefficients of the AAs particularly tryptophan (ε = 5,050 $M^{-1}cm^{-1}$) are large enough to absorb the energy from excited Ce^{3+} ions.

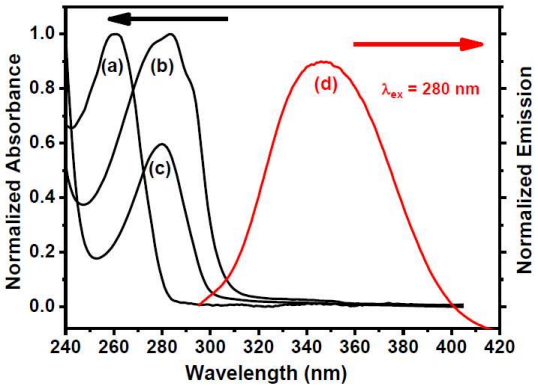

Fig. 5. Fig. 5. Uv-vis absorption spectra of (a) phenylalanine (b) tryptophan (c) tyrosine. (d) Emission spectrum of Ce^{3+}-doped $CaMoO_4$ nanocrystals.

Furthermore, a decrease in the Ce^{3+} emission intensity (at 340 nm) is observed for the Ce^{3+}-doped $CaMoO_4$ nanocrystals upon AAs addition, whereas the corresponding excitation spectra of Ce^{3+} ions are unaffected. These results clearly confirm occurrence of the energy transfer between Ce^{3+} ions and AAs. The excitation and emission spectra of Ce^{3+}-doped $CaMoO_4$ nanocrystals in the presence of AAs are shown in Fig. S3. We believe that the observed energy transfer is likely due to short separation between the Ce^{3+} and AAs present in the nanocrystals. Assuming that the Ce^{3+} ions are close to the surface of the nanocrystals, the maximum distance between Ce^{3+} ions and AAs is about 4 nm (distance of the SDS bilayer). This distance is within the FRET distance observed between dyes and Ln^{3+}-doped nanoparticles.[39] In fact for systems involving Ln^{3+} ions, the FRET distance is about 10 nm.[40] Moreover, the energy transfer between Ce^{3+} and AAs is supported by the decrease in the lifetime of Tb^{3+} emission from 1.97 ms to 934 µs in the presence of tryptophan. The corresponding values for tyrosine and phenylalanine are 507 and 277 µs, respectively (shown in Fig. S4). We emphasize that the difference in the lifetime values between the three aromatic amino acids can be used as a tool to differentiate between them.

To verify whether the selective quenching of Tb^{3+} luminescence upon addition of AAs to Ce^{3+}/Tb^{3+}-doped $CaMoO_4$ nanocrystals is reversible, we titrated the AAs complexed Ce^{3+}/Tb^{3+}-doped $CaMoO_4$ with 15 X 10^{-6} (M) ninhydrin. Upon addition of ninhydrin, there is a gradual increase in the Tb^{3+} luminescence suggesting that the quenching is reversible. It is clear from Fig. 6 that more than 90% of the initial intensity is recovered when tryptophan was used as quencher. The recovery studies for other two AAs (tyrosine and phenylalanine) are shown in Fig. S5 and S6. The luminescence quenching and recovery studies were performed for multiple cycles and the study reveals that the nanocrystals retained its initial luminescence intensity even after five cycles. The inset in Fig. 6 shows the PL intensity (550 nm) of the Ce^{3+}/Tb^{3+}-doped $CaMoO_4$ nanocrystals, when alternately 5 X 10^{-8} (M) tryptophan and 15 X 10^{-6} (M) ninhydrin were added for five regeneration cycles. The corresponding plots for the other two AAs (tyrosine and phenylalanine) are shown in Fig. S7 and S8, respectively. The observed luminescence recovery is likely due to the formation of complex between Aas and ninhydrin. The carbonyl group of the ninhydrin reacts with the amine group present in the amino acid and forms a Schiff base complex.[41] This is likely to change the absorption properties of the complex thus reducing the energy transfer efficiency between cerium ions and aromatic amino acids.

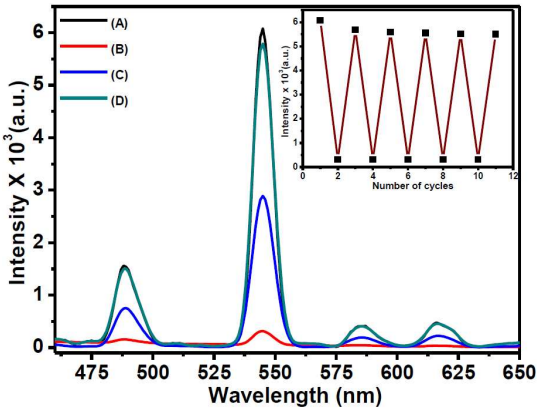

Fig. 6. PL spectra of AAs complexed-Ce^{3+}/Tb^{3+}-doped $CaMoO_4$ nanocrystals after the gradual addition of ninhydrin. (A) Luminescence spectra of Ce^{3+}/Tb^{3+}-doped $CaMoO_4$ nanocrystals (B) after addition of 5 X 10^{-8} (M) tryptophan solution (C) after addition of 5 X 10^{-6} (M) and (D) 15 X 10^{-6} (M) ninhydrin. Inset shows regeneration of intense luminescence signal of Tb^{3+} ion after alternate addition of 5 X 10^{-8} (M) tryptophan and 15 X 10^{-6} (M) ninhydrin.

To understand the nature of the quenching (static or dynamic), we have performed concentration dependent study (Stern-Volmer i.e. S-V plot). Interestingly, we observed a positive deviation in the S-V plot of Ce^{3+}/Tb^{3+}-doped $CaMoO_4$ nanocrystals in the presence of AAs as quencher (see Fig. S9) indicating the result of static component together with a dynamic component. The fractional intensity, I_0/I, is given by the product of both static and dynamic quenching.[42] Therefore

$I_0/I = (1+K_s[Q])(1+K_{sv}[Q]) = 1+K_1[Q] + K_2[Q]^2$ .....(1)

where $K_1 = (K_{sv} + K_s)$ and $K_2 = (K_{sv}$ X $K_s)$ are the dynamic and static quenching constants, respectively. Using the above equation, we measured the values of K*sv* and K*s*, which are found to be imaginary. For this reason, the above equation is not valid for the present case. Thus, the sphere of action static quenching model has been used. In accordance with this model, static quenching occurs only when the quencher molecules are very near to, or in contact with, fluorescent molecules at the

moment of its excitation. This is explained by the fact that only a certain fraction, W of the excited state is actually quenched by the collision mechanism. The rest fraction (1-W) of the excited states is deactivated almost instantaneously positioned in the proximity at the time the molecules are excited. Therefore, we have used the following modified form of the S-V equation.

$$I_0/I = \{1 + Ksv[Q]\}/W \quad \text{..... (2)}$$

The additional factor W is expressed as

$$W = \exp(-V[Q]) \quad \text{..... (3)}$$

Where V is the static quenching constant, and it represents an active volume element surrounding the excited state. Here, W depends on the quencher concentration [Q]. At high quencher concentrations, the S-V plot deviates from a linear character and equation 1 can be rewritten as

$$[1-(I/I_0)] / [Q] = Ksv\,(I/I_0) + (1-W) / [Q] \quad \text{..... (4)}$$

Fig. 7A shows the plot of $[1 - (I/I_0)]/[Q]$ versus I/I_0 for Ce^{3+}/Tb^{3+}-doped $CaMoO_4$ nanocrystals in the presence of AAs. By calculating the slope and intercept, the K_{sv} and V values are obtained. The dynamic and static quenching constant values for Ce^{3+}/Tb^{3+}-doped $CaMoO_4$ nanocrystals in the presence of tryptophan are 2.4 X 10^5 M^{-1} and 12.1 X 10^5 M^{-1}, respectively. The corresponding values for tyrosine and phenylalanine are listed in the Table S1 in the supporting information. The sensitivity of the nanocrystals is evaluated using 3σ/k (where σ is the standard deviation of the blank measurements (n= 7), k is the slope of the linear calibration curve) and is found to be 2.09 X 10^{-8} (M), 2.72 X 10^{-7} (M), 9 X 10^{-6} (M) for tryptophan, tyrosine and phenylalanine, respectively. For comparison, the linear range and detection limit (LOD) obtained from our method are listed in Table S2 (shown in the Supporting Information) along with the corresponding values obtained from some other methods. It is clear from the data that the AAs detection via lanthanide-doped nanocrystals is comparable to other methods.

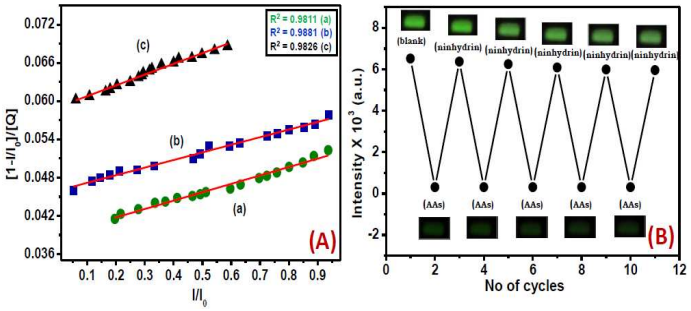

Fig. 7. (A) Plot of $[1 - (I/I_0)]/[Q]$ vs I/I_0 for Ce^{3+}/Tb^{3+}-doped $CaMoO_4$ nanocrystals in the presence of (a) tyrosine, (b) tryptophan and (c) phenylalanine. (B) PL quenching and recovery cycles from the Ce^{3+}/Tb^{3+}-doped $CaMoO_4$ nanocrystals deposited glass slide upon successive immersion of the slide into AAs and ninhydrin solutions respectively. The corresponding digital images are also shown.

To examine the feasibility of the developed nanocrystals for use in a sensing device, the nanoparticles were deposited onto a 2D surface and tested. Briefly, the negatively charged Ce^{3+}/Tb^{3+}-doped $CaMoO_4$ nanoparticles were deposited onto a commercially available positively charged glass slide. The slides were dried and immersed into a solution containing 5 X 10^{-8} (M) AAs. The PL emission of Tb^{3+} ions decreased when in contact with AAs solution. Subsequently, the PL was recovered by immersing the same glass slide into 15 X 10^{-6} M ninhydrin solution. The immersion cycles were repeated for more than five times and observed that the slides were active up to five cycles for AAs detection, and thereafter observed a slight decrease in the luminescence efficiency. The corresponding snapshots of the ON and OFF states of the green luminescence after immersing the device into ninhydrin and AAs solutions, respectively, are shown in Fig. 7B. A presentation of the above experiment is shown in Fig.8.

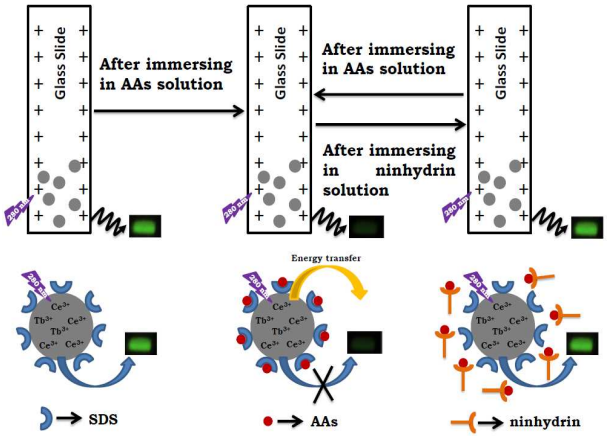

Fig.8 Schematic illustration of the attachment of nanocrystals on a positively charged glass slide and the luminescence changes of the same after dipping into AAs solution followed by immersing into ninhydrin solution.

Conclusions

Water dispersible SDS coated Ce^{3+}/Tb^{3+}-doped $CaMoO_4$ nanocrystals were prepared by microwave procedure. Upon Ce^{3+} (280 nm) excitation, Ce^{3+}/Tb^{3+}-doped $CaMoO_4$ nanocrystals show strong emission at 540 nm along with weak emissions near 488, 585 and 620 nm characteristics if Tb^{3+} ions. The emission intensities were selectively quenched upon addition of AAs like tryptophan, tyrosine and phenylalanine. This is attributed to the reduction in the efficiency of energy transfer from Ce^{3+} to Tb^{3+} ions caused by strong absorption of the Ce^{3+} energy by AAs. Thus the resonance energy transfer (RET) serves as a tool to selectively detect AAs upto nanomolar concentration. This luminescence quenching is very selective as the addition of other analytes (essential/non-essential amino acids, metal ions and molecules) hardly affected the emission intensity of the Tb^{3+} ions emission. Moreover, the detection of AAs was found to be reversible with the addition of ninhydrin. More than 90% of the initial intensity of the Tb^{3+} was recovered upon ninhydrin solution. Moreover, the selectivity and recoverability of the nanocrystals is tested on a 2D surface, which suggests that the material is suitable for device fabrication. This work may provide a novel strategy to fabricate a device for the detection of different amino acids.

Acknowledgements

VM thanks the Department of Science and Technology (DST) India, Council for Scientific and Industrial Research (CSIR) and IISER-Kolkata for the funding. CH and TS thank IISER-Kolkata and UGC respectively for their scholarship.

Notes and references

a Department of Chemical Sciences, Indian Institute of Science Education and Research (IISER), Kolkata, Mohanpur, West Bengal 741252, India. Fax: 91-33-25873020; Tel: +91(0)9007603474; E-mail: mvenkataramanan@yahoo.com

†Electronic Supplementary Information (ESI) available. Quantum Efficiency, Interference Study, Emission spectra of Ce^{3+}-doped $CaMoO_4$ nanocrystals, Decay Analysis, Recovery Study, Cycle, Stern-Volmer plot, Table of Quenching Constants, comparative study]. See DOI: 10.1039/c000000x/

1 R. Wu and T. B. McMahon, *J. Am. Chem. Soc.,* 2008, **130**, 12554-12555.

2 J. P. Gallivan and D. A. Dougherty, *Proc. Natl. Acad. Sci.,* 1999, **96**, 9459-9464.

3 S. K. Burley and G. A. Petsko, *Science*, 1985, **229**, 23-28.

4 J.C. Ma and D. A. Dougherty, *Chem. Rev*., 1997, **97**, 1303-1324.

5 D. A. Dougherty, Science, 1996, 271, 163-168.

6 N. P. Johns, J. Johns, S. Porasuphatana, P. Plaimee and M. T. Sae. J. *Agric. Food Chem.,* 2013, **61**, 913-919.

7 S. Burkhardt, D. X. Tan, L. C. Manchester, R. Hardeland and R. J. Reiter, *J. Agric. Food Chem.,* 2001, **49**, 4898-4902.

8 B. L. Williamson, A. J. Tomlinson, P. K. Mishra, G. J. Gleich and S. Naylor, *Chem. Res. Toxicol*. 1998, **11**, 234-240.

9 J. H. Gaddum, H. O. Schild, G. F. Somers and G. A. Stewart, *Analyst,* 1950, **75**, 530-550.

10 E. Boyland, E. P. Abraham, G. G. Newton, W. E. van Heyningen, J. Duckworth, D. Herbert and S. J. Folley, *Annu. Rep. Prog. Chem.,* 1950, **47**, 285-372.

11 R. A. Farishian and J. R. Whittaker, *J. Invest. Dermat*., 1980, **74**, 85-89.

12 A. Huijser, A. Pizzella and V. Sundstrom, *Phys. Chem. Chem. Phys*. 2011, **13**, 9119-9127.

13 M. P. A. Ebert, M. Korc, P. Malfertheiner and C. Rocken, *J. Proteome Res*., 2006, **5**, 19-25.

14 S. Kumar, J. Huang, J. R. Cushnir, P. Spanel, D. Smith and G. B. Hanna, *Anal. Chem*., 2012, **84**, 9550-9557.

15 A. Bornot, U. Bauer, A. Brown, M. Firth, C. Hellawell and O. Engkvist, *J. Med. Chem*., 2013, **56**, 1197-1210.

16 K. Deng, S. Lin, L. Zhou, Y. Li, M. Chen, Y. Wang and Y. Li, *PLoS One*, 2012, **7**, 49434

17 A. Laviano, A. Cascino, M. Muscaritoli, F. Fanfarillo and F. F. Rossi, *Adv. Exp. Med. Biol*., 2003, **527,** 363-366.

18 T. Sakata, G. Ferdous, T. Tsuruta, T. Satoh and S. Baba, *Pathol. Int*., 2009, **59**, 7-18.

19 N. Duraker, A. C. Naci and N. Jencler, *Eur. J. Surg. Oncol.*, 2002, **28**, 844-849.

20 K. Deng, L. Y. Zhou, S. R. Lin, Y. Li, M. Cheng, Q. M. Geng and Y. W. Li, *J. Dig. Dis*., 2013, **14,** 299-304.

21 X. Yu, L. Luo, Y. Wu, X. Yu, Y. Liu, X. Yu, X. Zhao, X. Zhang, L. Cui, G. Ye, Y. Le and J. Guo, *Med. Oncol*., 2013, **30**, 365.

22 a) D. A. Skoog, F. J. Holler and T. A. Nieman, *Principles of Instrumental Analysis, 5th ed.; Saunders College Publishing: Philadelphia, PA*, 1992; b) 30 C. Mueller, J.R. Fonseca, T.M. Rock, S. K. Etschmann, P. S. Kopplin, *J. Chromatogr. A,* 2014, **1324**, 109-114.

23 Y. Zhou and J. Yoon, *Chem. Soc. Rev*., 2012, **41**, 52-67.

24 a) O. Lioubashevski, V. I. Chegel, F. Patolsky, E. Katz and I. Willner, *J. Am. Chem. Soc*., 2004, **126**, 7133-7143; b) J. Gao, J. Fu, C. Lin, J. Lin, Y. Han, X. Yu and C. Pan, *Langmuir,* 2004, **20**, 9775-9779.

25 a) D. R. Bae, W. S. Han, J. M. Lim, S. Kang, J. Y. Lee, D. Kang and J. H. Jung, *Langmuir*, 2010, **26**, 2181-2185; b) L. Li and B. Li, Analyst, 2009, **134**, 1361-1365.

26 R. C. Carvalho, A. Mandil, K. P. Prathish, A. Amine and C. M. A. Brett, *Electroanalysis*, 2013, **25,** 903-913.

27 D. P. S. Negi and T. I. Chanu, *Nanotechnology*, 2008, **19**, 465503-7.

28 J. S. Lee, P. A. Ulmann, M. S. Han and C. A. Mirkin, *Nano Lett.*, 2008, **8,** 529-533.

29 L. F. Yuan, Y. J. He, H. Zhao, Y. Zhou and P. Gu, *Chinese Chem. Lett.*, 2014, **25,** 995-1000.

30 X. Wang, J. Wu, F. Li and H. Li, *Nanotechnology*, 2008, **19,** 205501 (8pp)

31 a) F. Wang and X. Liu, *Acc. Chem. Res*., 2014, **47**, 1378−1385; b) R. Komban, R. Beckmann, S. Rode, S. Ichilmann, A. Kühnle, U. Beginn and M. Haase, *Langmuir*, 2011, **27**, 10174–10183. T.Montini, A. Speghini, L. De Rogatis, B. Lorenzut,M. Bettinelli, M. Graziani and P. Fornasiero, *J. Am. Chem. Soc.,* 2009, **131**, 13155. F. Pandozzi, F. Vetrone, J.-C. Boyer, R. Naccache, J. A. Capobianco, A. Speghini and M. A. Bettinelli, *J. Phys. Chem. B,* 2005, **109**, 17400.

32 a) J.C. G. Bünzli, S. V. Eliseeva, *Chem. Sci*., 2013, **4**, 1939-1949; b) B. Voβ, J. Nordmann, A. Uhl, R. Kombana and M. Haase, *Nanoscale*, 2013, **5**, 806–812; C. Feldmann, M. Roming, K. Trampert, *Small*, 2006, 2, 1248-1250; J. Chen, Q. Meng, S. May, M. Berry, C..Lin, *J. Phys. Chem. C*, 2013, **117**, 5953-5962. Cross, A. M., May, S., van Veggel, F., Berry, M, *J. Phys. Chem. C*, 2010, **114**, 14747-14747.

33 a) N. J. J. Johnson, A. Korinek, C. Dong and F. C. J. M. van Veggel, *J. Am. Chem. Soc*., 2012, **134**, 11068−1107; b) S. V. Eliseeva , J.-C. G. Bünzli, *Chem. Soc. Rev*., 2010, **39**, 189 – 227.

34 a) X. D. Wang and O. S. Wolfbeis, *Chem. Soc. Rev*., 2014, **43**, 3666-3761; b) A. Sedlmeier, D. E. Achatz, L. H. Fischer, H. H. Gorris and O. S. Wolfbeis, *Nanoscale*, 2012, **4**, 7090-7096; c) L. H. Fischer, G. S. Harms and O. S. Wolfbeis, *Angew. Chem. Int. Ed*., 2011, **50**, 4546-4551.

35 a) F. Wang, D. Banerjee, Y. Liu, X. Chen, X. Liu, *Analyst*, 2010, **135**, 1839; b) N. M. Idris, M. K. G. Jayakumar, J. Zhang, P. C. Ho, R. Mahendran, Y. Zhang, *Nature Medicine* 2012, **18**, 1580-1585; c) L. Y. Ang, M. E. Lim, L. C. Ong, Y. Zhang, *Nanomedicine*, 2011, **6**, 1273-1288; d) G. K. Das, N. J. J. Jonson, J. Cramen, B. Blasiak, P. Latta, B. Tomanek and F. C. J. M. van Veggel, *J. Phys. Chem. Lett*., 2012, **3**, 524-529; e) G. Chen, T. Y. Ohulchanskyy, S. Liu, W. C. Law, F. Wu, M. T. Swihart, H. Ägren and P. N. Prasad, *ACS Nano*, 2012, **4**, 2969–2977; f) T. Liu, L. Sun, Y. Qiu, J. Liu, F. Li, L. Shi and O. S. Wolfbeis, *Microchim. Acta*, 2014, **181**, 1073-9; g) G. Jiang, J. Pichaandi, N. J. J. Johnson, R. D. Burke and Frank C. J. M. van Veggel, *Langmuir*, 2012, **28**, 3239−3247; h) Y. Yang, Q. Shao, R.

Deng, C. Wang, X. Teng, K. Cheng, Z. Cheng, L. Huang, Z. Liu, X. Liu, and B. Xing, *Angew. Chem. Int. Ed*., 2012, **51**, 3125-3129;

36 L. Zhao, J. Peng, M. Chen, Y. Liu, L.Yao, W. Feng and F. Li, *ACS Appl. Mater. Interfaces*, 2014, **6**, 11190−11197.

37 C. Hazra, T. Samanta, A. V. Asaithambi and V. Mahalingam, *Dalton Trans*., 2014, **43**, 6623–6630.

38 S. Pan, R. Deng, J. Feng, S. song, S. Wang, M. Zhu and H. Zhang, *CrystEngComm*, 2013, **15**, 7640-7643; J. Meijer, L. Aarts, B. van der Ende, T. Vlugt and A. Meijerink, *Phys. Rev. B: Condens. Matter Mater. Phys.,* 2010, **81**, 35107; P. Ghosh, A. Kar and A. Patra, *Nanoscale*, 2010, **2**, 1196-1202; K. Riwotzki, H. Meyssamy, H. Schnablegger, A. Kornowski, and M. Haase, *Angew. Chem. Int. Ed*., 2001, **40**, 573-576.

39 E. R. Trivedi, S. V. Eliseeva, J. Jankolovits, M. M. Olmstead, S. Petoud and V. L. Pecoraro, *J. Am. Chem. Soc*., 2014, **136**, 1526−1534; H. S. Killian, A. Meijerink and G. Blasse, *J. Lumin*., 1986, **35**, 155-161; R. Visser, P. Dorenbos, C. W. E. van Eijk, A. Meijerink, G. Blasse and H. W.den Hartog, *J. Phys.: Condens. Matter*, 1993, **5**, 1659-1680; A. Meijerink, H. Jetten and G. Blasse, *J. Solid. State Chem*., 1988, **76**, 115-123.

40 a) P. R. selvin and J. E. Hearst, *Proc. Nail. Acad. Sci*., 1994, **91**, 10024-10028; b) L. L. Li, P. Ge, P. R. Selvin and Yi Lu, *Anal. Chem*., 2012, **84**, 7852-7856; c) P. Ge and P. R. Selvin, *Bioconjugate Chem*., 2008, **19**, 1105- 1111.

41 M. Friedman, *J. Agric. Food Chem.* 2004, **52**, 385−406.

42 J. R. Lakowicz, *Principles of Fluorescence Spectroscopy, 2nd ed.; Kluwer Academic/Plenum publishers*: New York, 1999.

Graphical abstract